

The Design and Characterization of a Novel Piezoelectric Transducer-Based Linear Motor

Jeremy A. Palmer, *Member, IEEE*, Brian Dessent, *Member, IEEE*, James F. Mulling, Tim Usher, Edward Grant, *Senior Member, IEEE*, Jeffrey W. Eischen, *Member, IEEE*, Angus I. Kingon, and Paul D. Franzon, *Senior Member, IEEE*

Abstract—Before microminiature robots can be realized, new direct drive micromotor systems must be developed. In this research, a linear motor system for a miniature jumping robot was desired. However, current systems must display better force/torque characteristics than is currently available. This paper deals with the design, construction, and testing, of a macro-scale, unidirectional, direct drive linear piezomotor that operates like an inchworm. It uses a parallel arrangement of unimorph piezoelectric transducers, in conjunction with passive mechanical latches, to perform work on a coil spring. Experimental results showed that the linear piezomotor achieved a maximum no-load velocity of 161 mm/s, and a blocked force of 14 N, at a drive signal frequency of 100 Hz. Thereafter, back slip in the latch assembly restricted the forward motion. Based on the results obtained with the macro-level linear piezomotor, it is concluded that smaller direct drive piezomotor designs based on unimorph piezoelectric transducers are achievable. System scalability will be addressed in a future publication.

Index Terms—Direct drive motors, linear piezomotor, passive latches, piezoelectric transducers.

I. INTRODUCTION

RECENT mechatronic systems research at North Carolina State University, Raleigh, has concentrated on developing miniature jumping robots. A review of relevant literature in the natural sciences revealed the mechanisms inherent in animals with jumping locomotion [1]. These include actuation, energy storage, and rapid release [1]. Accordingly, a scalable, unidirectional linear piezoelectric motor (piezomotor) was created that incorporates these mechanisms to perform the work of jumping in a mobile robotic platform. The following novel features of the linear piezomotor design are discussed in this paper.

Manuscript received August 22, 2003; revised December 28, 2003. This work was supported in part by the Defense Advanced Research Projects Agency (DARPA), MTO Office Distributed Robotics Initiative under Contract N3998-98-C3536.

J. A. Palmer was with North Carolina State University, Raleigh, NC 27695 USA. He is now with Sandia National Laboratories, Albuquerque, NM 87185-0958 USA (e-mail: japalme@sandia.gov).

B. Dessent was with North Carolina State University, Raleigh, NC 27695 USA. He is now with the University of California, Berkeley, CA 94720 USA (e-mail: brian@dessent.net).

J. F. Mulling and A. I. Kingon are with the Department of Materials Science and Engineering, North Carolina State University, Raleigh, NC 27695 USA (e-mail: jfmullin@eos.ncsu.edu; angus_kingon@ncsu.edu).

T. Usher is with the Department of Physics, California State University, San Bernardino, CA 92407 USA (e-mail: tusher@csusb.edu).

E. Grant and P. D. Franzon are with the Department of Electrical and Computer Engineering, North Carolina State University, Raleigh, NC 27695 USA (e-mail: egrant@eos.ncsu.edu; paulf@ncsu.edu).

J. W. Eischen is with the Department of Mechanical and Aerospace Engineering, North Carolina State University, Raleigh, NC 27695 USA (e-mail: eischen@eos.ncsu.edu).

Digital Object Identifier 10.1109/TMECH.2004.828647

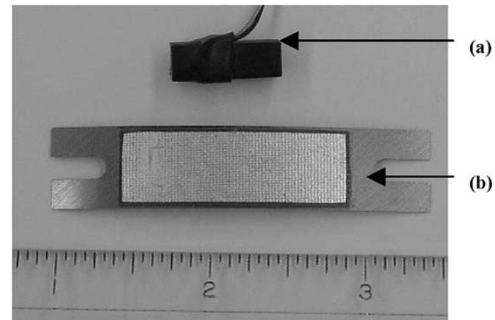


Fig. 1. Two types of piezoelectric transducers. (a) PZT stack. (b) THUNDER stressed unimorph.

At the heart of the linear piezomotor is a high-stiffness parallel arrangement of stressed unimorph piezoelectric transducers known as THUNDER transducers. THUNDER transducers are capable of larger strains [2] relative to laminated stack transducers and, thus, do not require external structures to amplify displacement. The design includes a passive latch system to control the energy transfer and rapid release. The passive latch has the advantages of simplicity and compactness when compared to actively controlled clamp systems. In addition, experimental data is reported to document the performance and limitations of the piezomotor prototype.

Bizzigotti [3], Zhang and Zhu [4], and King [5], have made important contributions to the evolution of simple, scalable, nonultrasonic linear piezomotors. These groups attempted to harness the high forces generated by laminated piezoceramic lead-zirconate-titanate (PZT) “stack” transducers. They proved that stack thickness was directly proportional to the final displacement achieved. Because PZT stacks typically produce displacements of approximately 1 μm per layer, complex mechanical amplification systems were necessary to boost the submillimeter strains [4], [5]. Future microrobot applications will impose a severe size limitation on piezomotor design, making external amplification methods infeasible. For this reason, high-displacement THUNDER stressed unimorph transducers offer a more practical alternative in the context of miniaturization [2].

THUNDER transducers are compliant and exhibit a flexural displacement many times greater than the strains generated by stacks. A THUNDER unimorph piezoelectric transducer is composed of a thin laminate of composite ferroelectric driver and sensor material (piezoceramic), and aluminum bonded to a steel substrate using a polyimide adhesive at elevated temperature [6]. Photographs of a THUNDER and a stack transducer appear in Fig. 1. The mismatch in the coefficients of thermal expansion in the piezoceramic and substrate materials

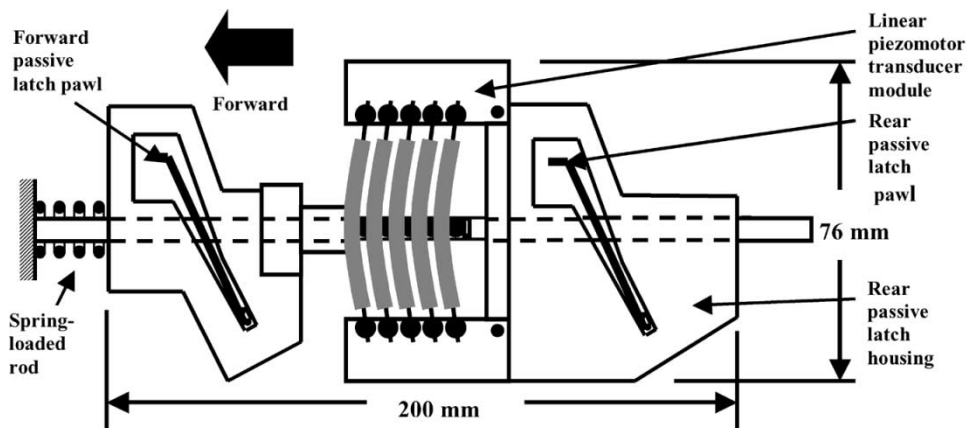


Fig. 2. Prototype linear piezomotor (sideview, showing THUNDER transducers mounted in parallel and passive latches, not to scale).

introduces residual stresses in the composite structure. As a result, the THUNDER exhibits a curved or bowed-edge profile. When a voltage is applied to the THUNDER transducer, the radius of curvature of the substrate lessens, affecting the biaxial deformation and the stiffness of the system [8], [9]. When the voltage is removed, the transducer returns to its original shape. Previous experimentation proved that the performance of THUNDER transducers was highly dependent upon their stiffness and end conditions [9]. In order to increase the stiffness of the prototype linear piezomotor, the THUNDER transducers were arranged in parallel, such that each transducer deflected the same amount when the actuation voltage was applied. This design made the individual transducer stiffness accumulative. The linear piezomotor developed in this program used rectangular THUNDER transducers because the geometry, stiffness, and end mounting conditions were consistent and verifiable [7], [9]. Furthermore, they were compatible with a modular piezomotor design. THUNDER transducers are supplied in various sizes, thereby allowing the scalability issue to be addressed in the future. The research reported in this paper was conducted on the macroscale.

Figs. 2 and 3 depict the linear piezomotor prototype. The prototype assembly contains two passive latches that are joined to a module containing 20 mechanically coupled THUNDER transducers. Note that in Fig. 2, the bearings that hold the transducers were designed to allow the transducers to rotate and translate simultaneously [9]. Passive latches are incorporated in the linear piezomotor to control the displacement of the transducer module, and to rapidly release energy stored in the spring. Passive latches are mechanical diodes that permit motion of the linear piezomotor in one direction only. They are found in many industrial products; see [12] and [13]. A review of the latch design literature showed that a passive latch pawl naturally rotates to an open position when moving in the forward (nonbinding) direction (see Fig. 2), allowing forward motion of the linear piezomotor with minimal friction. The opposite is true when the latches are operated in the reverse direction, which results in a braking action. In contrast to active clamp mechanisms, the simple passive latch design is more cost-effective in terms of control system circuitry and algorithms. The operating sequence of the piezomotor assembly shown in Fig. 2, including the passive latches and transducer module, is as follows: 1) voltage is applied to the transducers, causing the module to *contract* and the rear latch to move forward while 2) the forward latch binds,

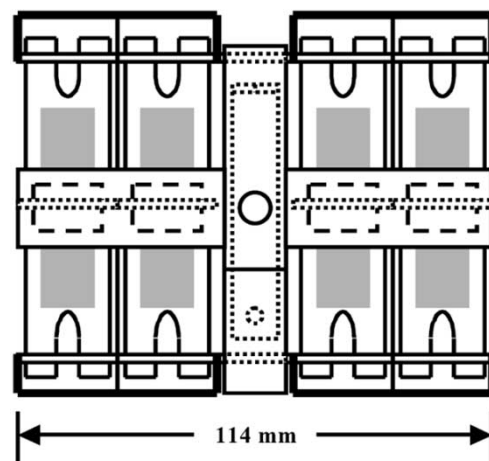


Fig. 3. Prototype linear piezomotor (front view, not to scale).

forming an anchor, which pulls the piezomotor forward. Upon removal of the voltage, the transducers relax, and the module *expands*, pushing the forward latch ahead. In this mode, the rear latch binds and blocks any reverse displacement. This cyclic (nonreversible) inchworm motion drives the linear piezomotor against the spring, performing useful work. The stored energy is rapidly released by simultaneously rotating the latch pawls to the open position using a simple trigger mechanism (not shown).

II. LINEAR PIEZOMOTOR ANALYSIS

There are three parts to the linear piezomotor system analysis. First, the equivalent stiffness of the piezomotor is derived based on dynamic equivalence. Other associated stiffness relationships are also detailed. Second, an empirical model is derived to predict the blocked force of the THUNDER transducer (this analysis is separate from that of the latch assemblies). Third, a static equilibrium analysis is carried out on the passive latch assembly, to establish its operating principles.

From equivalent dynamic systems theory, K_{eq} is the sum of the stiffnesses of n individual transducers operating in parallel. This is due to the fact that the transducers deflect the same amount. The relationship is expressed as follows:

$$K_{eq}(V) = k_1(V) + \dots + k_{n-1}(V) + k_n(V). \quad (1)$$

The stiffness k_i produced by an individual transducer is a function of the applied voltage, reflects the tendency for stiffness to increase in the steel substrate as it flexes during actuation [8].

The blocked force of a THUNDER transducer module is classified in two ways: 1) the *free mass* type, F_1 , denotes a load level at which all flexural displacement of the module ceases, and more importantly and 2) the *actuator* blocked force, F_2 , (a qualitative measure), which causes a static deflection that is equal the no-load flexural displacement of the transducer module, δ_0 . The actuator blocked force reduces the elastic rebound of the transducer module to approximately zero. When the load applied to the linear piezomotor reaches this level, all apparent forward motion stops. The value of F_2 is calculated from the product of δ_0 and the zero-potential equivalent stiffness, $K_{eq}(0)$

$$F_2 = \delta_0 K_{eq}(0). \quad (2)$$

Blocked force types F_1 and F_2 are predicted empirically from a plot of the recorded experimental data, transducer displacement versus load, over a range of applied voltages. The procedure for determining F_1 and F_2 is discussed in greater depth in a later section.

The following static analysis illustrates the operational principle of the passive latch and was useful in the empirical design of the pawl. Fig. 4 shows a static equilibrium model for the pawl of the passive latch mechanism. At the instant shown, motion in the negative x direction is about to occur. The force F is due to the contact of the latch housing and the pawl; its horizontal component, F_x (not shown) acts at point C . Preload force Q , provided by a fitted spring, maintains the contact between the pawl and the rod, at an angle θ relative to the rod centerline. Contact between the edges of the hole in the pawl and the rod cause the binding forces N and N' . This contact also causes the corresponding friction forces F_f and F'_f , respectively. Assuming that the weight of the pawl, W , acts at the centroid as indicated, static equilibrium in the x and y planes yield the following instantaneous equations for the binding forces:

$$\sum F_x = \mu_s N + \mu_s N' - F \sin \theta + Q \sin \theta = 0 \quad (3a)$$

$$\sum F_y = N - N' - W + F \cos \theta - Q \cos \theta = 0 \quad (3b)$$

$$N = \frac{1}{2} \left[(F - Q) \left(\frac{\sin \theta}{\mu_s} - \cos \theta \right) + W \right]$$

$$N' = \frac{1}{2} \left[(F - Q) \left(\frac{\sin \theta}{\mu_s} + \cos \theta \right) - W \right]. \quad (3c)$$

From (3c), it is noted that although preload force is necessary to maintain the pawl in contact with the rod, excessive preload works against the piezomotor by increasing friction in the forward (nonbinding) direction. Pawl thickness was designed by experiment. As the ratio of the pawl thickness to rod diameter approaches unity, the experimental results show that the binding action diminishes. This is due to the rod deflecting under the action of the forces acting on the system. Displacement loss due to relative motion between the rod and pawl in the direction indicated in Fig. 4 is referred to as back slip. Back slip occurs during the binding operation of the latch. Several factors contribute to

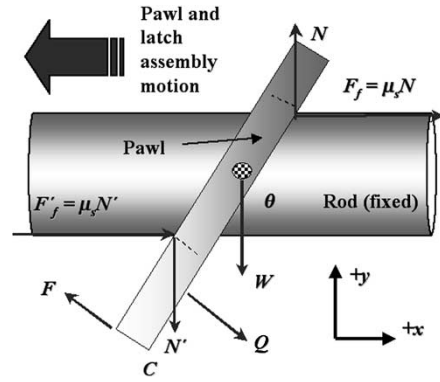


Fig. 4. Free body diagram of the impending motion of a passive latch pawl.

the measurable level of back slip. In addition to simple sliding losses between the rod and pawl, they include deflection of the latch housing, rod, and pawl; contact deformation between the rod and pawl, and losses incurred during rotation of the pawl from the open configuration to the closed or binding position. Of the back slip mechanisms cited, rotation of the pawl is the most significant contributor. At the onset of forward motion of the piezomotor as indicated in Fig. 2, the latch housing and pawl separate near the point where the preload is applied. The pawl subsequently rotates clockwise about the lower point of contact with the rod. Rotation continues past the point where the coefficient of static friction between the rod and pawl is overcome, and relative sliding motion occurs. Motion ceases when the friction forces and the restoring force provided by the pawl preload spring balance each other. In order for the latch to bind during the next contraction sequence of the THUNDER transducer module, the pawl must rotate counterclockwise, returning to its starting position. This return rotation is facilitated by the rearward motion of the latch housing, which constitutes the back slip. Linear piezomotor operation fails when back slip equals the transducer flexural displacement.

III. EXPERIMENTAL PROCEDURE

A test rig was designed and constructed to allow a set of experiments to be carried out on the linear piezomotor, e.g., a set of calibrated coil springs could be easily introduced to carry out load experiments. The test rig, shown in Fig. 5, was planned to be a standard apparatus for characterizing the performance of any new linear piezomotor design. A computer program was devised for linear piezomotor characterization [9]. This program recorded performance data including actuator velocity and blocked force versus drive signal frequency, and energy density in joules per kilogram. Two linear variable differential transformers (LVDTs) were connected between the body of the linear piezomotor and the frame of the test rig. Attaching the LVDTs in this manner allowed the relative motion of the latches to be measured. This data was required to calculate the displacement losses associated with the passive latches. All measurements were carried out for varying load conditions. The results obtained allowed the performance of the linear piezomotor to be compared against similar piezomotor technologies [10], [11]. Experimental procedures were developed to allow the performance of the prototype to be evaluated. The data extracted: 1)

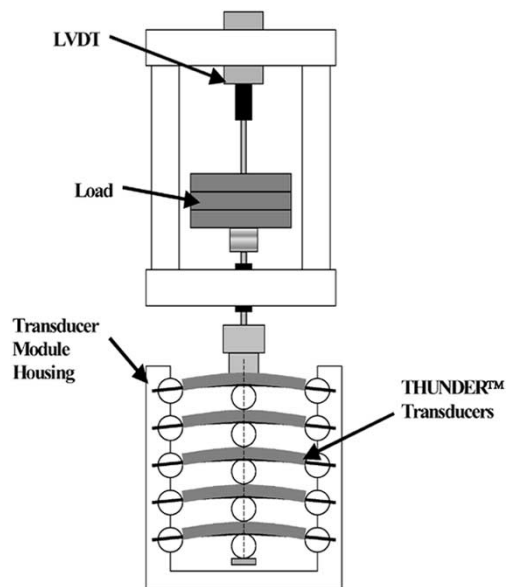


Fig. 5. Characterization test rig showing a piezomotor transducer module under test.

aided the development of empirical models of the THUNDER transducer module, e.g., this data contributed to determining the equivalent stiffness and actuator blocked force; 2) yielded the velocity of the linear piezomotor; and 3) supported the evaluation of performance under load, e.g., the data allowed latch slip losses to be evaluated. In each of the three experimental procedures, the linear piezomotor was controlled by a square wave input signal generated by a PC-based LabVIEW program. The maximum amplitude of the control signal applied to the linear piezomotor transducers was 480 V. The motion of the transducer module is converted to a voltage by the calibrated LVDT transducers on the test rig. Data was recorded from the LVDT with a virtual digital multimeter (DMM) interface in LabVIEW. The stylus column of the test apparatus was incrementally loaded to a maximum of approximately 10 N for each test. At each load increment, a sequence of voltages was applied to the THUNDER transducer module. The corresponding stylus position, measured by the LVDT, was recorded and displayed on the virtual DMM. The blocked force was derived from the plot shown in Fig. 6, stylus position versus load. The slope of each graph plotted for a series of trials is the reciprocal of stiffness, or compliance. In Fig. 6, the difference in slopes of each graph indicates that the piezoelectric transducer stiffness varies with the applied voltage.

To record velocity, a LVDT was connected to the rear passive latch assembly shown in Fig. 2. A digital storage oscilloscope captured output voltage readings from the LVDT and plotted them with respect to time. The velocity of the linear piezomotor is the product of the recorded no-load displacement and drive signal frequency. Load characteristics were derived by running the prototype against a calibrated coil spring. To monitor back slip, it was necessary to introduce a second LVDT into the test rig. Joined to the forward passive latch assembly, it was used to derive the relative motion between the forward and rear latches. Under varying load conditions, oscilloscope traces of the two

TABLE I
TRANSDUCER MODULE CHARACTERIZATION RESULTS

Parameter	Symbol	Value	Units
Actuator blocked force	F_2	19.8	N
No-load flexural displacement	δ_0	401	μm
Zero potential equivalent stiffness	$K_{eq}(0)$	49.2	N/mm
480-volt equivalent stiffness	$K_{eq}(480)$	49.4	N/mm
Zero potential single transducer stiffness	$k_t(0)$	2.5	N/mm
480-volt single transducer stiffness	$k_t(480)$	2.7	N/mm

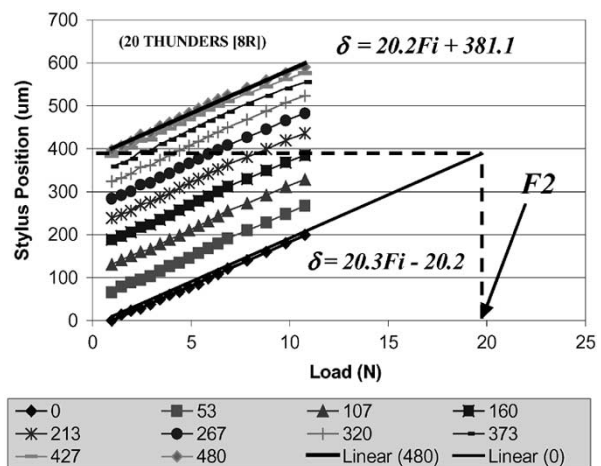


Fig. 6. Stylus position versus load and voltage for a transducer module containing 20 Type 8R THUNDER transducers.

LVDT signals were analyzed to determine the relative displacement between the latches.

IV. RESULTS

Table I summarizes the results obtained from the linear piezomotor characterization trials using the experimental procedures outlined above. Plots of the empirical model, based on (2) are shown in Fig. 6. From the information derived from the model, an actuator blocked force of 19.8 N was predicted. Similarly, a corresponding no-load flexural displacement of 401 μm (determined by the difference of the y -intercepts of the 0 and 480 V trend lines) is also predicted. The stiffness of the complete THUNDER transducer module, i.e., twenty transducers mounted in parallel, was found by experiment, measured at 0 and 480 V. At these voltages, the transducer module stiffness was shown to be 49.2 and 49.4 N/mm, respectively. The stiffness value for a single 8R THUNDER was also obtained at the 0 and 480-V levels used earlier, see Table I. The stiffness values were shown to be 2.5 and 2.7 N/mm, respectively, approximately 1/20 of that of the collective stiffness of the complete module. Further experimentation with the linear piezomotor, at various frequency settings, produced the data that was necessary to determine the maximum velocity

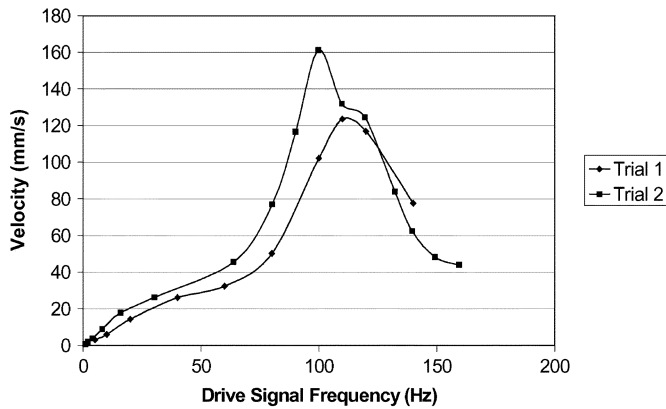


Fig. 7. Linear piezomotor velocity versus drive signal frequency.

and the maximum load. Obtaining experimental blocked force results allowed comparisons to be drawn between that and the theoretical blocked force results calculated earlier. This dual approach of experimentation and analysis allowed the system losses to be described.

A plot of no-load velocity versus drive signal frequency is illustrated in Fig. 7. The results of two independent trials indicate that the maximum velocity of the linear piezomotor is achieved at approximately 100 Hz. The peak velocity was 161 mm/s. The no-load velocity test revealed that the value of displacement steps incrementally increased as the test progressed. Interpretation of the data showed that the transfer of linear momentum from the rear latch assembly to the forward half of the linear piezomotor was the cause of the increasing displacement. The largest blocked force observed in the trials was 14 N at 50 Hz. This experimentally generated value was 30% lower than the derived actuator blocked force. There are a number of inherent loss mechanisms in the linear piezomotor design, either or all of which can contribute to reducing the net displacement of the linear piezomotor to zero. The experiments showed that zero displacement occurs when the load level approximates the actuator blocked force.

Examination of the latch displacement waveforms produced by the LVDT transducers shows that measurable amounts of back slip exist in the latches. In fact, a percentage of the THUNDER transducer module flexural displacement is lost every cycle, due to one or both of the latches sliding backward prior to binding. Here, displacement efficiency is defined as the ratio of net forward displacement to transducer flexural displacement per cycle. Figs. 8 and 9 show how displacement efficiency and the output flexural displacement per cycle, or "step displacement" (d_{TH}) of the THUNDER transducers erodes, and how back slip intensifies with increasing load. Under these conditions, the maximum blocked force produced by the linear piezomotor is limited by the displacement efficiency of the latches. Note that in Fig. 9, negative latch slip denotes relative motion in the forward direction. Energy density of the linear piezomotor is expressed as the product of the no-load flexural displacement of the THUNDER transducer module and the maximum observed blocked force; divided by the mass of the linear piezomotor. Module displacement is used to avoid bias from inertial effects in the prototype displacement

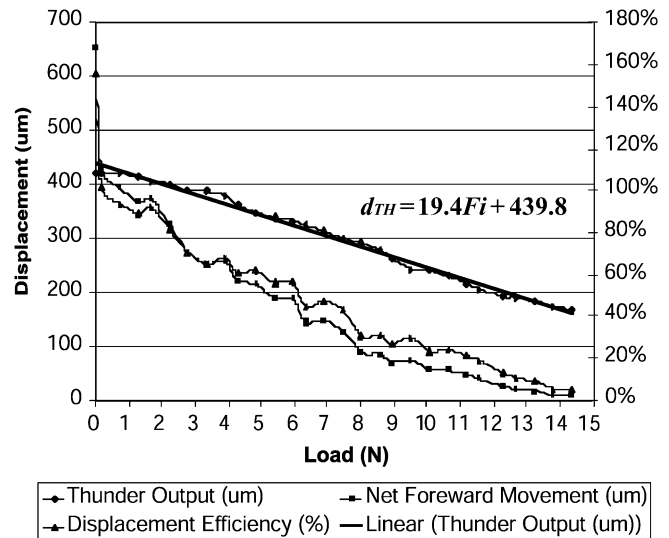


Fig. 8. Linear piezomotor displacement and displacement efficiency versus load.

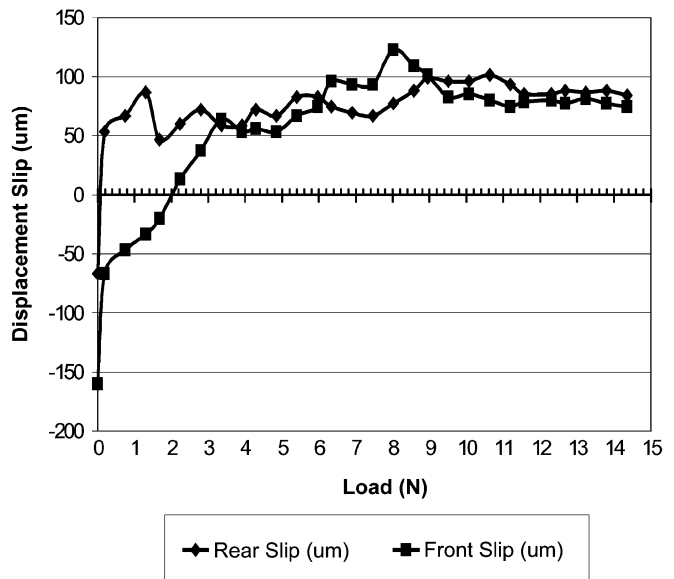


Fig. 9. Linear piezomotor latch slip versus load.

data. Based on the data reported earlier, and with a prototype mass of 850 grams, the energy density of the linear piezomotor is calculated to be 0.0066 J/kg. Multiplying the energy density by the drive signal frequency yields the power density. At 100 Hz, the linear piezomotor power density is 0.66 W/kg.

V. CONCLUSION

This research investigated how to design and construct a unique linear piezomotor, one based on THUNDER stressed unimorph transducer technology, and develop an understanding of its operating principles. The long-term goal of the research is the construction of micro-scale linear piezomotors for jumping robots. First, experiments were conducted into storing enough energy to produce a force large enough to give jumping motion, but with a macro-scale linear piezomotor. The maximum force generated by the linear piezomotor was determined by testing

it against a calibrated spring load. Experiments determined the maximum velocity versus frequency, maximum blocked force versus frequency, energy density, and latch slip losses, all of which varied with an increasing load. This paper catalogues the results obtained from these characterization trials, and from a supporting theoretical analysis, carried out on the design of the transducer module and passive latch assembly. Experimentation revealed that the linear piezomotor produced a maximum no-load linear velocity of 161 mm/s at a transducer drive signal frequency of approximately 100 Hz. This result includes inertial effects on the latch assemblies. Under test, the linear piezomotor achieved a blocked force of 14 N, at which point the forward displacement of the piezomotor and the back slip losses inherent in the latch design cancelled each other out, i.e., the relative motion was zero. This back slip curtails the force output of the linear piezomotor, meaning that the blocked force produced did not reach the actuator blocked force of approximately 20 N estimated by an empirical model. Considering that the 20 N actuator blocked force was qualitative (one chosen by the design team), the 14 N value obtained during the linear piezomotor experiments is encouraging. Designing a linear piezomotor to generate a specific actuator blocked force entailed selecting an appropriate number of THUNDER transducers to assemble in parallel. In the trials described above, the recorded blocked force of 14 N translates to a displacement efficiency of less than 40%, and a step displacement of approximately 150 μm (see Fig. 8). Subtracting this number from the no-load flexural displacement reported in Table I yields a revised, or compensated displacement value of 251 μm . Given the individual zero potential transducer stiffness of 2.5 N/mm, this displacement value may be substituted into the following:

$$F_2' = pk_{i0} \delta_0' \quad (4)$$

where, F_2' is the desired actuator blocked force, p is the number of transducers, k_{i0} denotes the zero potential transducer stiffness, and δ_0' is the compensated no-load flexural displacement. Solving (4) for p reveals the necessary number of transducers. Using this method, 32 transducers are needed to compensate for back slip and realize the original objective load capacity of 20 N. It follows that the linear piezomotor presented here utilizes a greater number of parallel transducers than many stack-based systems to generate comparable levels of force [4], [5]. However, the modular design based on scalable THUNDER transducers and passive latches eliminates extraneous displacement amplification and clamp control systems required with stacks. This represents a key advantage that may facilitate implementation of nonultrasonic linear piezomotors on the millimeter scale.

ACKNOWLEDGMENT

The authors thank the North Carolina State University Center, Raleigh, for Robotics and Intelligent Machines (CRIM), the Departments of Electrical and Computer Engineering, Materials Science and Engineering, and Mechanical and Aerospace Engineering, and lastly, JMC Tool and Machine, Inc., for their contributions to this research.

REFERENCES

- [1] R. F. Chapman and A. Joern, *A Biology of Grasshoppers*. New York: Wiley, 1990.
- [2] K. M. Mossi, G. V. Selby, and R. G. Bryant, "Thin-layer composite unimorph ferroelectric driver and sensor properties," *Mater. Lett.*, vol. 35, pp. 39–49, 1998.
- [3] R. A. Bizzigotti, "Electromechanical Translation Apparatus," U.S. Patent 3 902 085, 1975.
- [4] B. Zhang and Z. Zhu, "Developing a linear piezomotor with nanometer resolution and high stiffness," *IEEE/ASME Trans. Mechatron.*, vol. 2, pp. 22–29, Mar. 1997.
- [5] W. Xu and T. G. King, "Piezomotors using flexure hinged displacement amplifiers," *Inst. Elect. Eng. Colloq. Innovative Actuators Mechatron. Syst.*, vol. 11, pp. 1–5, 1995.
- [6] S. A. Wise, "Displacement properties of rainbow and thunder piezoelectric actuators," *Sens. Actuators*, vol. A69, pp. 33–38, 1998.
- [7] J. M. Gere and S. P. Timoshenko, *Mechanics of Materials*, 4th ed. Boston, MA: PWS-Kent, 1997.
- [8] W. C. Young, *Roark's Formulas for Stress and Strain*, 6th ed. New York: McGraw-Hill, 1989.
- [9] J. F. Mulling *et al.*, "High displacement piezoelectric actuators: Characterization at high load with controlled end conditions," in *Proc. 2000 12th IEEE Int. Symp. Applications Ferroelectrics*, vol. 2, 2000, pp. 745–748.
- [10] J. W. Judy, D. L. Polla, and W. P. Robbins, "A linear piezoelectric stepper motor with submicrometer step size and centimeter travel range," *IEEE Trans. Ultrason., Ferroelect., Freq. Contr.*, vol. 37, pp. 428–437, Sept. 1990.
- [11] K. Yen and G. Roig, "Linear piezoelectric step motors," *IEEE Proc. 1990 Southeastcon*, vol. 1-C1, pp. 21–24, 1990.
- [12] J. Drake, "Bar Latch for Single-Hand Operation," U.S. Patent 5 853 168, 1998.
- [13] A. S. Goul, "Fast clamp," U.S. Patent 4 874 155, 1989.



Jeremy A. Palmer (M'94) received the B.S. degree in mechanical engineering from the University of Connecticut, Storrs, in 1994, the M.S. degree in mechanical engineering, and the Ph.D. degree in mechanical and electrical engineering from North Carolina State University, Raleigh, in 1999 and 2002, respectively.

He is a Senior Member, Technical Staff, Sandia National Laboratories, Albuquerque, NM. His research interests include meso-scale mechatronic systems engineering, microfabrication, rapid proto-

typing, and photonics.



Brian Dessent (M'02) received the B.S. degree in both electrical engineering and computer science from North Carolina State University, Raleigh, in 1998, and the M.S. degree in electrical engineering from the University of California, Berkeley in 2003.



James F. Mulling received the B.S. degree in materials science and engineering from North Carolina State University, Raleigh, in 1998, where he is currently pursuing a M.S. degree, also in materials science and engineering, conducting microrobotics and ferroelectric materials research at the North Carolina State University Center for Robotics and Intelligent Machines (CRIM).



Tim Usher received the Ph.D. degree from the University of South Carolina, Columbia, in 1990.

He is currently a Professor of Physics at California State University, San Bernardino.



Edward Grant (SM'02) received the B.S. (Hons.) degree in mechanical engineering from the Dundee College of Technology, Dundee, U.K., in 1969; the M.E. degree from the University of Sheffield, Sheffield, U.K., in 1972; and the Ph.D. degree in computer science from the University of Strathclyde, Glasgow, U.K., in 2000.

He is the Director of the Center for Robotics and Intelligent Machines (CRIM) at North Carolina State University, Raleigh, and Associate Professor of Electrical and Computer Engineering. His research inter-

ests include knowledge-based control of robotic and dynamic systems, evolutionary and biorobotics, e-textiles, and search and rescue robots.

Dr. Grant is a Chartered Engineer (C.Eng.), a Fellow of the Institution of Mechanical Engineers (F.I.Mech.E.), and an Associate Editor of the *International Journal of Robotics and Autonomous Systems*.



Jeffrey W. Eischen (M'87) received the B.S. degree in civil engineering from the University of California, Los Angeles in 1978; and the M.S. and Ph.D. degrees in applied mechanics from Stanford University, Stanford, CA, in 1981 and 1986, respectively.

He is currently an Associate Professor of Mechanical and Aerospace Engineering at North Carolina State University, Raleigh. His research interests include linear and nonlinear finite element analysis of multibody kinematics/dynamics/control, fabric mechanics, and stress analysis in microelectronic

devices.



Angus I. Kingon received the B.S. (Hons.) degree from the University of the Witwatersrand, South Africa, in 1975 and the M.S. (*cum laude*) and Ph.D. degrees from the University of South Africa, Pretoria in 1978 and 1981, respectively.

He is currently a Professor of Materials Science and Engineering at North Carolina State University, Raleigh and a Professor associated with the Department of Business Management. His research interests include ferroelectric and piezoelectric thin films and bulk materials, dielectric materials, gate dielectrics, sensors and actuators, memory devices, RF and microwave materials, embedded passive devices, and microelectronic packaging. He is author of approximately 220 research publications.

Dr. Kingon is a Fellow of the American Ceramic Society and an Associate Editor of several journals.



Paul D. Franzon (SM'02) received the Ph.D. degree from the University of Adelaide, Adelaide, Australia, in 1988.

He is a Professor of electrical and computer engineering at North Carolina State University, Raleigh. He has also worked at AT&T Bell Laboratories, DSTO Australia, Australia Telecom, and Communications, Ltd. His research interests include the design of complex systems incorporating VLSI, MEMS, advanced packaging and nanotechnology.

Dr. Franzon received the National Science Foundation Young Investigators Award in 1993, and was elected to the North Carolina State University Academy of Outstanding Teachers in 2001.